

## A Ethic statement

Our method is a general-purpose inference-time optimization framework designed to maximize task-specific reward functions. The ethical implications of its use are inherently tied to how the reward function is defined. While this flexibility allows for beneficial applications—enabling faster and more targeted generation aligned with desirable outcomes—it also raises the potential for misuse if the reward function encodes harmful or biased objectives. Therefore, the responsibility for ethical deployment lies in the careful design and oversight of the reward specification.

## B Experiment details

### B.1 Computational resource

Our implementation is built using the PyTorch framework. The experiments are conducted on 2 machines: Ubuntu 20.04 machine equipped with an Intel(R) Xeon(R) Gold 6348 CPU @ 2.60GHz with 112 cores, 384 GB RAM, and NVIDIA GeForce RTX 4090 GPUs; Ubuntu 22.04 machine equipped with an Intel(R) Xeon(R) Gold 6230R CPU @ 2.10GHz with 104 cores, 256 GB RAM, and NVIDIA GeForce RTX 4090 GPUs. Each experiment is run individually on an NVIDIA GeForce RTX 4090 GPU.

### B.2 Task detail

We introduce the setting of experiments and diffusion models we used. For **Mixture of Gaussian**, we constructed the two datasets generated from the mixture of gaussians. Dataset 1 is generated from 1 region of Gaussians and Dataset 2 is generated from 2 region of the islands as you can see on the Figure 2(a). After pre-training two diffusion models on each dataset, we guide sampling at inference time by providing the distance to a target goal as a reward, encouraging generation toward the desired goal state. For **OGBench Maze**, we adopted the task setups from [19], running 5 sparse reward navigation tasks in each environment, each can take hundreds of steps to accomplish. The model is trained on standard dataset collected by noisy expert policy that repeatedly reaching randomly sampled goals. At test time, the model is required to generate proper plan using guidance from value function. For **Sudoku**, the basic setting is adopted from IRED [8], where the diffusion model is trained on SAT-Net dataset with 31 to 42 provided samples [29] and tested on harder RRN dataset [18] with 17 to 28 provided samples. For **Pixel Maze**, the basic setting is adopted from T-SCEND [35], where the dataset are generated by maze-dataset [12], and the diffusion model is trained with Maze sizes of  $4 \times 4$  to  $6 \times 6$  and tested with size of  $11 \times 11$  to  $15 \times 15$ . For **Molecule Generation**, the basic setting is adopted from EDM [11]. The diffusion model is trained to generate 3D molecular geometries using the QM9 dataset [20], which contains approximately 130k small molecules, each with up to 9 heavy atoms. We utilized the standard splits of this dataset for training, validation, and testing. For **Text-to-Image generation**, we use Stable Diffusion v1.5—a widely adopted text-to-image diffusion model—as our pretrained backbone.

**Verifiers.** For **OGBench Maze**, we employ a soft verifier that scores each generated plan based on the proportion of collision-free states throughout the trajectory and the proximity to the goal at the end of the trajectory. For **Sudoku**, we use the ratio of correct answer that matches the ground truth label. For **Pixel Maze**, we use weighted sum of Precision, Recall, F1 score with rate of success score which indicates whether the path reaches the goal without passing the wall. For **Molecule Generation**, we use the Negative Log-Likelihood (NLL) to evaluate the generated molecular structures. For **Text-to-Image generation**, we use three verifier scores: compressibility [2], aesthetic [22], and human preference score [33].

**Evaluation metrics.** For **OGBench Maze**, we used the success rate (whether the planned trajectory reaches to the goal or not) of the actual rollouts from the generated trajectory plans. For **Sudoku**, we use the ratio of correct answer that matches the ground truth label. For **Pixel Maze**, we use success score (0 or 1) which indicates whether the path reaches the goal without passing the wall. For **Molecule Generation**, we use molecule stability (0 or 1), the proportion of generated molecules for which all atoms are stable. For **Text-to-Image generation**, we use three evaluation metrics: compressibility [2], aesthetic [22], and human preference score [33]—which correspond to specific verifiers, respectively.

### B.3 Baseline detail

We compare ABCD (ours) to several representative methods capable of inference-time scaling.

**Base Diffusion** is the most basic baseline, which generates samples without any additional computation during inference. When a differentiable value function is available, we include **Classifier Guidance** [5] as a base diffusion baseline.

**Best-of-N(BoN)** generates  $N$  samples from the pre-trained diffusion model and returns the sample with the highest reward score according to the verifier.

**Search over Paths (SoP)** [16] is a recently proposed method that performs inference-time scaling by alternating backward(noising) and forward(denoising) transitions in the denoising space. Starting from  $M$  particles, the method perturbs each particle with  $K$  different noise moving to  $\Delta f$  steps backward, resulting in  $M \times K$  expanded candidates (expansion). Each of these is then denoised forward for  $\Delta b$  steps. After reaching the new states, each particles are scored using a verifier, and the top  $M$  are selected to continue (selection). This process is repeated until the particles reach  $t = 0$ , with the constraint that  $\Delta f < \Delta b$  to ensure overall forward progression.

**Diffusion Beam Search (BS)** [17] is another baseline that performs inference-time search over denoising trajectories. Starting from  $M$  initial particles, the method branches each into  $K$  candidate continuations every  $p$  denoising steps, and retains the top  $M$  candidates based on reward estimates. This beam-style selection continues until the denoising process reaches  $x_0$ . Our implementation is inspired by [17], with necessary modifications for our setting.

**Sequential Monte Carlo Diffusion (SMC)** [24] is a sampling-based method that employs Sequential Monte Carlo (SMC) to steer diffusion trajectories toward high-reward regions [31]. Inspired by the Feynman-Kac Steering Diffusion framework (FKD) [24], it begins with an initial set of  $N$  proposal particles and performs iterative resampling every  $p$  steps during the denoising process, using importance weights defined by tailored potentials. These potentials are designed to approximate the reward-weighted posterior distribution  $p(\mathbf{x})p(c | \mathbf{x})$  (where the reward encodes the target condition), effectively guiding particle evolution toward desirable outputs. Our implementation follows the general structure of FKD, with modifications to accommodate our conditional generation setting. Specifically, we define  $p(c | \mathbf{x})$  using the task-specific verifier score to guide the sampling process. As this is a sampling-based approach, we select the highest-scoring particle from the final set of  $N$  samples drawn from the guided distribution.

ABCD’s inference-time termination is controlled by three hyperparameters: the percentage threshold, the maximum iteration bound (`max_iter`), and the persistence parameter  $\kappa$ . The percentage threshold defines the minimum fraction of top- $K$  particles that must originate from the zero *go-back* noise level in order to raise a termination flag. Inference is terminated once this condition holds for  $\kappa$  consecutive iterations. We scale inference-time computation by varying both the percentage threshold and  $\kappa$ , which jointly determine the strictness of the stopping condition. Additionally, we adjust `max_iter` to cap the total number of iterations. As these hyperparameters increase, the termination criterion becomes more conservative, typically leading to longer inference time and improved performance through extended refinement.

Unless otherwise specified, in both SoP, BS and SMC, since we have reward function defined on  $\mathbf{x}_0$  space, the reward evaluations at each step  $\mathbf{x}_t$  are performed using a predicted clean sample  $\hat{\mathbf{x}}_0(\mathbf{x}_t)$  (approximation of  $\mathbb{E}_{\mathbf{x}_0 \sim p_{\text{pre}}}[\mathbf{x}_0 | \mathbf{x}_t]$ ), which is then passed into the verifier [14, 15, 24]. With this choice, we get the intermediate reward  $r(\mathbf{x}_t, c) = r(\mathbf{x}_0 = \hat{\mathbf{x}}_t, c)$ . This ensures that reward signals are consistent across trajectories and noise levels.

### B.4 MoG experiment detail

We constructed two Mixture of Gaussians datasets: Dataset 1 has 36 modes concentrated in a single region, while Dataset 2 distributes 36 modes across two regions (18 modes each). Two separate diffusion models were pretrained on each datasets using 100 denoising steps. In each experiment, we initialize with  $M = 2$  particles sampled from the prior, and use  $K = 4$  distinct noise samples to guide the particles backward.



## B.5 MoG result detail

### B.5.1 Small *go-back* levels vs. large *go-back* levels

As shown in Figure 10, small *go-back* levels effectively guide the particle toward the goal when navigating within a single region landscape. However, in the two-regions scenario (Figure 11), small *go-back* levels struggle to move particles across regions to reach the goal. By contrast, large *go-back* levels significantly improve cross-region transitions.

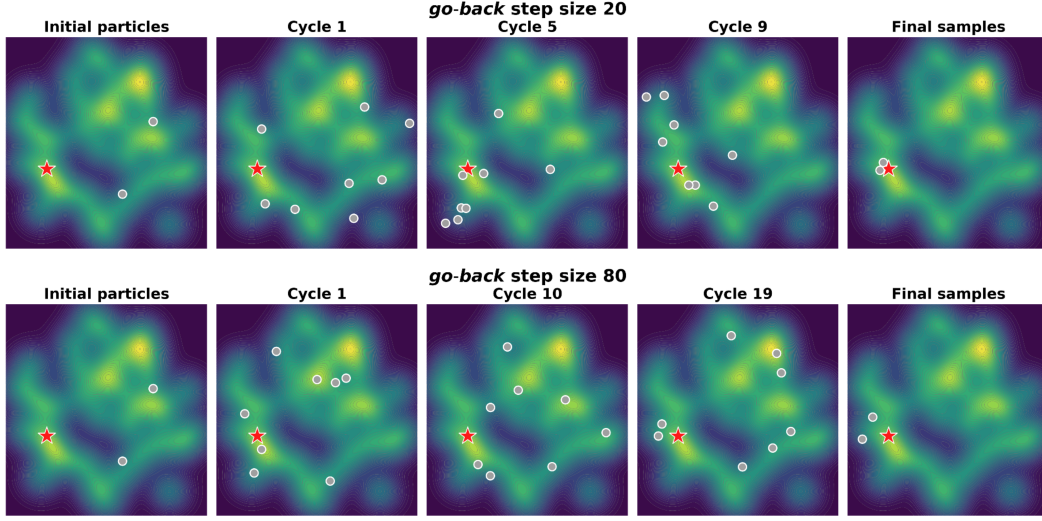


Figure 10: Compare different *go-back* step size on task 1.

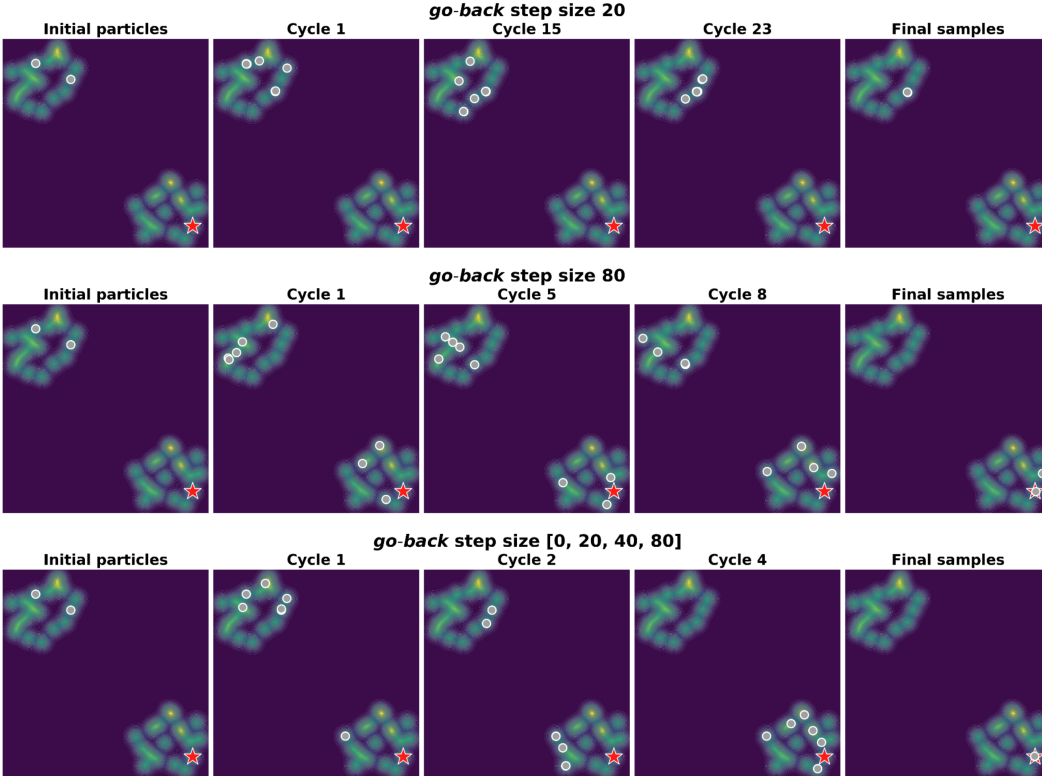


Figure 11: Compare single and multiple *go-back* step size on task 2.

### B.5.2 Single *go-back* levels vs. multiple *go-back* levels

After leveraging the large *go-back* to traverse between regions, switching to small *go-back* becomes advantageous for shifting from exploration to exploitation. This transition enables fine-grained goal-oriented refinement, as demonstrated in Figure 11. All instances begin from an initial incorrect prediction, requiring additional correction during inference. *go-back* = 20 fails to escape the initial cluster of modes, whereas *go-back* = 80 enables transitions across regions but refines inefficiently. Our method combines coarse transitions to explore distant regions and fine adjustments for local refinement, enabling faster and more effective inference time adjustment.

### B.6 OGBench Point Maze experiment detail

All methods were evaluated under the same setup, using 32 particles to ensure a fair comparison. For **SoP**, we used  $M = 4$  and  $K = 8$  in Maze Giant, and  $M = 1$  and  $K = 32$  in Maze Large. **BS** used  $M = 8$  and  $K = 4$  in both mazes, with a lookahead estimator [17] to have a better predicted  $\hat{\mathbf{x}}_0(\mathbf{x}_t)$  with value guidance. **SMC** [24] was implemented with `POTENTIAL TYPE = "sum"`,  $\lambda = 0.1$  and used  $N = 32$  particles in both mazes. **ABCD** was configured with  $N = 32$ ,  $K = 2$  and  $J = 16$  in Maze Giant and  $N = 32$ ,  $K = 1$  and  $J = 32$  in Maze Large. The adaptive terminal condition was set once more than 90% of top- $K$  particles consistently originated from the zero noise level over  $\kappa$  consecutive steps. We used  $\kappa = 30$  in Maze Giant and  $\kappa = 5$  in Maze Large. All methods used a base diffusion model trained with 256 denoising steps. ABCD employed jumpy denoising with a jump length of 10.

To scale inference compute, we increased the branching-and-selection frequency  $p$  for BS and SMC. For BoN, we scaled by increasing  $N$ . For SoP, we varied the step size for back-and-forth moves, as smaller steps incur higher compute due to finer-grained trajectory updates. For ABCD, we scaled by increasing the number of `max_iter`. Inference time was measured as the average time required to generate and execute a single plan in the environment.

## B.7 OGBench Point Maze result

Figure 6 compares the performance using an adaptive guidance scheme that increases guidance as the diffusion step  $t$  approaches 0. For reference, the performance of all methods under the standard guidance scheme is reported in Table 3 and Table 4. ABCD consistently outperforms all baselines, and is the only method to achieve a perfect success rate within the given compute budget.

**Table 3:** Comparison of inference-time strategies in OGBench Point Maze Giant.

| Inference Method | Add. Compute                 | Performance | Inference wall clock time (sec.) |
|------------------|------------------------------|-------------|----------------------------------|
| Base Diffusion   | No add                       | 12±13       | 41.02                            |
| BoN              | N = 32                       | 36±15       | 43.12                            |
|                  | N = 64                       | 54±22       | 45.34                            |
|                  | N = 96                       | 48±18       | 45.38                            |
|                  | N = 128                      | 60±24       | 48.64                            |
|                  | N = 192                      | 64±15       | 53.78                            |
|                  | N = 288                      | 64±17       | 87.94                            |
|                  | N = 544                      | 76±20       | 169.98                           |
| SoP              | $\Delta f=200, \Delta b=100$ | 40±9        | 59.12                            |
|                  | $\Delta f=100, \Delta b=50$  | 60±15       | 76.56                            |
|                  | $\Delta f=50, \Delta b=25$   | 86±13       | 88.06                            |
|                  | $\Delta f=40, \Delta b=20$   | 92±10       | 99.08                            |
|                  | $\Delta f=30, \Delta b=15$   | 94±9        | 108.84                           |
|                  | $\Delta f=20, \Delta b=10$   | 90±13       | 131.90                           |
|                  | $\Delta f=10, \Delta b=5$    | 94±13       | 181.94                           |
|                  | $\Delta f=6, \Delta b=3$     | 96±12       | 250.06                           |
|                  | $\Delta f=4, \Delta b=2$     | 86±9        | 342.94                           |
|                  | $\Delta f=2, \Delta b=1$     | 80±0        | 588.98                           |
| SMC              | $p = 50$                     | 28±20       | 52.52                            |
|                  | $p = 25$                     | 20±13       | 62.48                            |
|                  | $p = 20$                     | 20±13       | 67.20                            |
|                  | $p = 15$                     | 22±14       | 73.82                            |
|                  | $p = 10$                     | 22±11       | 90.82                            |
|                  | $p = 5$                      | 18±19       | 142.48                           |
| BS               | $p = 50$                     | 38±11       | 65.40                            |
|                  | $p = 20$                     | 30±10       | 92.30                            |
|                  | $p = 15$                     | 52±18       | 74.84                            |
|                  | $p = 10$                     | 46±16       | 122.08                           |
|                  | $p = 5$                      | 50±16       | 239.12                           |
|                  | $p = 1$                      | 72±16       | 1014.30                          |
| ABCD             | max_iter = 1                 | 82±11       | 12.70                            |
|                  | max_iter = 5                 | 94±9        | 34.02                            |
|                  | max_iter = 10                | 96±8        | 65.52                            |
|                  | max_iter = 15                | 96±8        | 85.98                            |
|                  | max_iter = 20                | 96±8        | 117.54                           |
|                  | max_iter = 25                | 96±8        | 138.04                           |
|                  | max_iter = 30                | 98±6        | 184.40                           |
|                  | max_iter = 35                | 100±0       | 202.58                           |
|                  | max_iter = 40                | 100±0       | 214.08                           |
|                  | max_iter = 45                | 100±0       | 271.68                           |
|                  | max_iter = 50                | 100±0       | 295.12                           |

**Table 4:** Comparison of inference-time strategies in OGBench Point Maze Large.

| Inference Method | Add. Compute                 | Performance | Inference wall clock time (sec.) |
|------------------|------------------------------|-------------|----------------------------------|
| Base Diffusion   | No add                       | 38±11       | 25.10                            |
| BoN              | N = 2                        | 62±11       | 28.88                            |
|                  | N = 4                        | 70±16       | 34.82                            |
|                  | N = 8                        | 80±9        | 41.58                            |
|                  | N = 16                       | 88±10       | 39.66                            |
|                  | N = 32                       | 94±9        | 41.74                            |
|                  | N = 64                       | 98±6        | 40.12                            |
| SoP              | $\Delta f=200, \Delta b=100$ | 64±15       | 58.22                            |
|                  | $\Delta f=100, \Delta b=50$  | 76±12       | 78.36                            |
|                  | $\Delta f=50, \Delta b=25$   | 86±9        | 92.52                            |
|                  | $\Delta f=40, \Delta b=20$   | 80±15       | 94.28                            |
|                  | $\Delta f=30, \Delta b=15$   | 92±10       | 94.32                            |
|                  | $\Delta f=20, \Delta b=10$   | 98±6        | 121.12                           |
|                  | $\Delta f=10, \Delta b=5$    | 96±8        | 158.48                           |
|                  | $\Delta f=6, \Delta b=3$     | 96±8        | 214.18                           |
|                  | $\Delta f=4, \Delta b=2$     | 98±6        | 285.60                           |
|                  | $\Delta f=2, \Delta b=1$     | 94±9        | 323.36                           |
| SMC              | $p = 50$                     | 84±8        | 44.82                            |
|                  | $p = 25$                     | 84±8        | 51.26                            |
|                  | $p = 20$                     | 82±11       | 50.92                            |
|                  | $p = 15$                     | 82±11       | 53.08                            |
|                  | $p = 10$                     | 76±15       | 61.40                            |
|                  | $p = 5$                      | 74±9        | 81.90                            |
| BS               | $p = 50$                     | 88±10       | 58.44                            |
|                  | $p = 20$                     | 88±10       | 60.50                            |
|                  | $p = 15$                     | 84±12       | 89.16                            |
|                  | $p = 10$                     | 90±13       | 115.64                           |
|                  | $p = 5$                      | 88±10       | 158.30                           |
|                  | $p = 1$                      | 94±9        | 801.42                           |
| ABCD             | J = 32                       | 100±0       | 10.52                            |

### B.7.1 OGBench Point Maze visualization

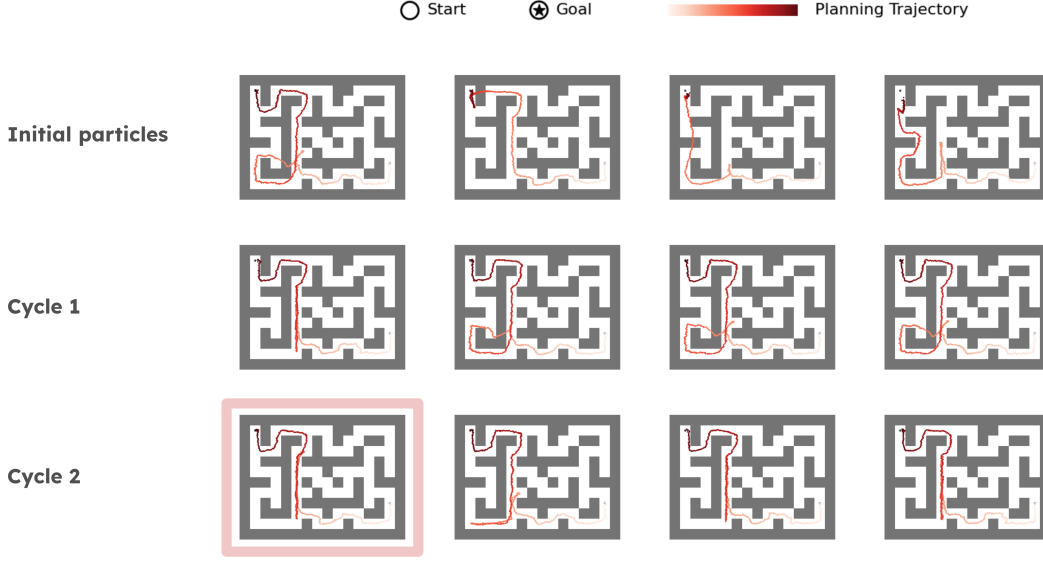


**Figure 12:** Visualization of the generated trajectories through cycle with ABCD. The figure highlighted with a red border indicates the selected plan for executing in the environment.

As shown in Figure 12, the initial trajectories proposed by jumpy denoising effectively capture a rough path from the start to the goal, yet contain noticeable invalid segments. Across subsequent cycles, Cyclic Diffusion Search progressively refines these trajectories by focusing on problematic regions and improves them toward viable plans. The highlighted plan selected for execution (red border) showcases ABCD’s capability to preserve the nearly-complete solution by leveraging Automatic Exploration-Exploitation Balancing mechanism.

### B.8 Sudoku experiment detail

Experiments were conducted on 335 Sudoku test instances, each containing between 17 and 28 provided digits. Reported accuracy reflects the average performance across the full test set. Inference time was measured as the average time required to generate a single sample, computed by dividing the total time taken to generate all 335 outputs by 335. The base diffusion model was trained using  $T = 50$  denoising steps. We follow the training configuration described in [35]. Each digit from 1 to 9 is represented as a one-hot vector, normalized, and passed through the diffusion model. During inference, the model outputs continuous predictions, which are then discretized by selecting the index with the highest predicted value as the final label.

To evaluate inference-time scaling strategies, each baseline was scaled along its primary computational axis while preserving its core algorithmic structure. **Base Diffusion** employed a single particle ( $N = 1$ ). **BoN** increased inference cost by evaluating models with  $N = 40, 480$ , and  $960$  particles. **BS** and **SoP** were implemented with  $M = 4$  and  $K = 10$ . In **BS**, inference-time compute was scaled by increasing the branching-and-selection frequency  $p$ . **SoP** additionally scaled computation by reducing the step sizes for forward and backward transitions,  $(\Delta b, \Delta f)$ . **SMC** used  $N = 40$  particles and scaled inference-time compute by adjusting the resampling frequency  $p$  across timesteps. Following the FKD framework [24], we set the POTENTIAL TYPE to “max” and  $\lambda = 100$  to enforce an optimization-style behavior. **ABCD (ours)** was configured with  $N = 10$ ,  $K = 10$ , and  $J = 5$ , corresponding to four non-zero *go-back* noise levels (10, 20, 30, 40) and one zero level. The adaptive terminal condition terminated inference when a specified percentage of top- $N$  particles consistently originated from the zero noise level for  $\kappa$  consecutive steps. We fixed `max_iter` to 100 and scaled ABCD’s inference time by varying both the persistence parameter  $\kappa \in \{1, 2, 3, 5, 10, 15, 20\}$  and percentage thresholds  $\in \{0.6, 0.8, 1.0\}$ . For fast denoising, ABCD employed five total inference steps, each performing a 10-step jump in the diffusion space. Please refer to Table 5 for detailed results.



## B.9 Sudoku result

We provide detailed results in Table 5 corresponding to the main Figure 4(Middle) presented in the main paper in this section. Additionally, Section B.9.1 visualizes the evolution of  $\mathbf{x}_0$  predictions across refinement cycles in the Sudoku task, illustrating how different *go-back* temperature step sizes affect the iterative denoising trajectory.

**Table 5:** Comparison of various inference-time strategies across compute and performance in the Sudoku harder test set setting (from 17 to 28 provided entities). For each method, inference-time compute was scaled by adjusting its primary control axis—such as branching frequency, resampling rate, or particle count—while preserving its core algorithmic behavior.

| Inference Method | Add. Compute                    | Accuracy         | Clock Time (sec.) | NFE   |
|------------------|---------------------------------|------------------|-------------------|-------|
| Base Diffusion   | No add                          | $0.35 \pm 0.1$   | 0.28              | 50    |
| BoN              | N = 40                          | $0.55 \pm 0.49$  | 0.29              | 2000  |
|                  | N = 480                         | $0.63 \pm 0.48$  | 0.68              | 24000 |
|                  | N = 960                         | $0.66 \pm 0.09$  | 1.32              | 48000 |
| SMC              | $p = 5$                         | $0.64 \pm 0.1$   | 0.3               | 2000  |
|                  | $p = 2$                         | $0.70 \pm 0.1$   | 0.31              | 2000  |
|                  | $p = 1$                         | $0.74 \pm 0.1$   | 0.32              | 2000  |
| BS               | $p = 5$                         | $0.65 \pm 0.46$  | 0.32              | 900   |
|                  | $p = 2$                         | $0.75 \pm 0.48$  | 0.40              | 1500  |
|                  | $p = 1$                         | $0.84 \pm 0.08$  | 0.54              | 2460  |
| SoP              | $\Delta f = 40, \Delta b = 20$  | $0.61 \pm 0.09$  | 0.41              | 2940  |
|                  | $\Delta f = 20, \Delta b = 10$  | $0.67 \pm 0.1$   | 0.46              | 3420  |
|                  | $\Delta f = 10, \Delta b = 5$   | $0.76 \pm 0.1$   | 0.51              | 3860  |
|                  | $\Delta f = 6, \Delta b = 3$    | $0.83 \pm 0.11$  | 0.52              | 3940  |
|                  | $\Delta f = 4, \Delta b = 2$    | $0.88 \pm 0.09$  | 0.55              | 4220  |
|                  | $\Delta f = 2, \Delta b = 1$    | $0.95 \pm 0.06$  | 0.65              | 4980  |
|                  | $\Delta f = 4, \Delta b = 3$    | $0.955 \pm 0.06$ | 0.99              | 8260  |
|                  | $\Delta f = 5, \Delta b = 4$    | $0.958 \pm 0.06$ | 1.14              | 9900  |
|                  | $\Delta f = 6, \Delta b = 5$    | $0.957 \pm 0.06$ | 1.33              | 11540 |
| ABCD             | percentage = 0.6, $\kappa = 1$  | $0.82 \pm 0.14$  | 0.24              | 1059  |
|                  | percentage = 0.8, $\kappa = 1$  | $0.90 \pm 0.1$   | 0.35              | 1667  |
|                  | percentage = 1.0, $\kappa = 1$  | $0.95 \pm 0.06$  | 0.45              | 2296  |
|                  | percentage = 1.0, $\kappa = 2$  | $0.97 \pm 0.05$  | 0.49              | 2607  |
|                  | percentage = 1.0, $\kappa = 3$  | $0.979 \pm 0.04$ | 0.55              | 2827  |
|                  | percentage = 1.0, $\kappa = 5$  | $0.986 \pm 0.03$ | 0.60              | 3205  |
|                  | percentage = 1.0, $\kappa = 10$ | $0.99 \pm 0.01$  | 0.75              | 3942  |
|                  | percentage = 1.0, $\kappa = 15$ | $0.995 \pm 0.01$ | 0.85              | 4499  |
|                  | percentage = 1.0, $\kappa = 20$ | $0.996 \pm 0.01$ | 0.92              | 5013  |

### B.9.1 Sudoku visualization showing that proper *go-back* is necessary

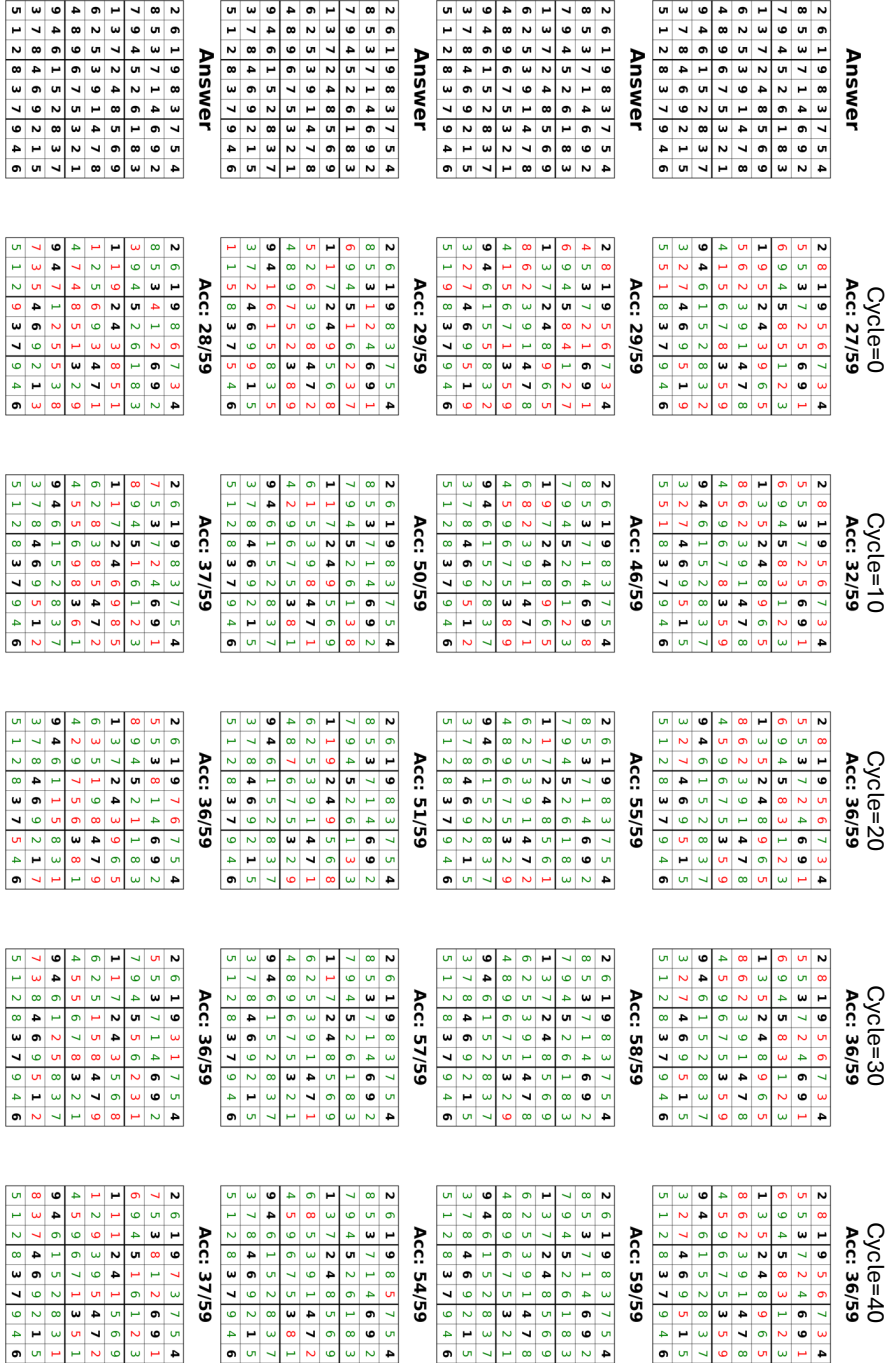


**Figure 13:** Visualization of  $x_0$  predictions across cycles for four *go-back* step sizes. The rightmost column corresponds to *go-back* 10, followed by 20, 30, and 40 in ascending order from right to left.

As shown in the visualization results for Sudoku in Figure 13, when the *go-back* noise level is set to 10, the  $x_0$  prediction remains unchanged despite repeated iterations failing to fix incorrect predictions. In contrast, with a noise level of 40, the  $x_0$  prediction appears to update randomly at each iteration altering even the correct ones, as if generating entirely new guesses without accumulating information from previous predictions. For noise levels 20 and 30—especially 20—we observed meaningful performance improvement across iterations, where incorrect predictions were corrected while correct ones were unchanged. These findings confirm that appropriately selecting the *go-back* noise level—both per task and per instance—is crucial for maximizing the benefits of inference-time iterative refinement.

## B.10 Pixel Maze experiment details

Experiments were conducted on 100 Pixel Maze test instances for each maze size (from 11 to 15). The reported success rate reflects the proportion of cases in which the generated trajectory successfully reaches the goal without crossing any walls. Inference time was measured as the average time required to generate a single sample, computed by dividing the total generation time for 100 samples by 100. The base diffusion model was pretrained using  $T = 50$  denoising steps. We follow the training configuration described in [35]. Both the maze layout (with walls encoded as 1 and empty spaces as 0) and the start/goal positions are represented as one-hot vectors and normalized before being passed into the diffusion model. During inference, the model produces continuous predictions, which are discretized by selecting the index with the highest value at each position, yielding the final binary path representation.

To assess inference-time scaling strategies, each baseline was scaled along its primary computational axis while preserving its core algorithmic behavior. **Base Diffusion** employed a single particle ( $N = 1$ ). **BoN** increased inference cost by using a larger number of particles  $N$ . **BS** and **SoP** were implemented with  $M = 4$  and  $K = 10$ . In **BS**, inference-time compute was scaled by increasing the branching and selection frequency  $p$ . In **SoP**, additional scaling was achieved by reducing the step sizes for forward and backward transitions,  $(\Delta b, \Delta f)$ . **SMC** used  $N = 40$  particles and scaled inference-time compute by varying the resampling frequency  $p$  over steps. Following FKD [24], we used POTENTIAL TYPE = “max” and set  $\lambda = 100$  to emphasize optimization behavior. **ABCD (ours)** was configured with  $N = 10$ ,  $K = 10$ , and  $J = 5$ , corresponding to four non-zero *go-back* noise levels (10, 20, 30, 40) and a zero level. The adaptive terminal condition terminated inference once a specified proportion of top- $N$  particles consistently originated from the zero noise level for  $\kappa$  consecutive iterations. We scaled ABCD’s inference time by varying  $\kappa \in \{1, 2, 3\}$  and percentage thresholds  $\in \{0.1, 0.2, 0.3, 0.6, 1.0\}$ . To ensure computational efficiency, ABCD employed ten denoising steps, each executing a 5-step jump in the diffusion process. Please refer to Table 6 for detailed results.

## B.11 Pixel Maze result

We provide detailed results corresponding to the main Figure 4(Left) presented in the main paper in Section B.11.1, and further demonstrate that the varying inference-time behavior—previously observed in the Sudoku setting—also holds in the Pixel Maze setting, as discussed in Section B.11.2

### B.11.1 Result table for Pixel Maze size = 15

This section provides a breakdown of the scaling factors we used, the performances and corresponding inference times for each method in Table 6.

**Table 6:** Comparison of various inference-time strategies across compute and performance in the Pixel Maze setting (size = 15). For each method, inference-time compute was scaled by adjusting its primary control axis—such as branching frequency, resampling rate, or particle count—while preserving its core algorithmic behavior.

| Inference Method | Add. Compute                   | Success rate    | clock Time (sec.) | NFE   |
|------------------|--------------------------------|-----------------|-------------------|-------|
| Base Diffusion   | No add                         | $0.02 \pm 0.13$ | 0.2               | 50    |
| BoN              | N = 20                         | $0.17 \pm 0.37$ | 1.87              | 1000  |
|                  | N = 40                         | $0.2 \pm 0.4$   | 2.67              | 2000  |
|                  | N = 80                         | $0.24 \pm 0.42$ | 5.46              | 4000  |
|                  | N = 160                        | $0.34 \pm 0.47$ | 10.52             | 8000  |
|                  | N = 200                        | $0.38 \pm 0.48$ | 13.0              | 10000 |
| SMC              | $p = 25$                       | $0.2 \pm 0.4$   | 3.21              | 2000  |
|                  | $p = 10$                       | $0.28 \pm 0.44$ | 3.61              | 2000  |
|                  | $p = 5$                        | $0.32 \pm 0.46$ | 4.58              | 2000  |
|                  | $p = 2$                        | $0.39 \pm 0.48$ | 6.58              | 2000  |
|                  | $p = 1$                        | $0.36 \pm 0.48$ | 10.31             | 2000  |
| BS               | $p = 4$                        | $0.25 \pm 0.43$ | 2.69              | 1020  |
|                  | $p = 3$                        | $0.32 \pm 0.46$ | 4.11              | 1180  |
|                  | $p = 2$                        | $0.39 \pm 0.48$ | 5.78              | 1500  |
|                  | $p = 1$                        | $0.61 \pm 0.48$ | 10.79             | 2460  |
| SoP              | $\Delta f = 40, \Delta b = 20$ | $0.25 \pm 0.43$ | 4.05              | 2940  |
|                  | $\Delta f = 20, \Delta b = 10$ | $0.54 \pm 0.49$ | 4.98              | 3420  |
|                  | $\Delta f = 10, \Delta b = 5$  | $0.76 \pm 0.42$ | 6.35              | 3860  |
|                  | $\Delta f = 8, \Delta b = 4$   | $0.85 \pm 0.35$ | 6.69              | 3900  |
|                  | $\Delta f = 6, \Delta b = 3$   | $0.91 \pm 0.28$ | 7.08              | 3940  |
|                  | $\Delta f = 4, \Delta b = 2$   | $0.95 \pm 0.21$ | 8.43              | 4220  |
|                  | $\Delta f = 2, \Delta b = 1$   | $0.98 \pm 0.13$ | 12.42             | 4980  |
| ABCD             | percentage = 0.1, $\kappa = 1$ | $0.17 \pm 0.37$ | 0.65              | 310   |
|                  | percentage = 0.2, $\kappa = 1$ | $0.44 \pm 0.49$ | 1.22              | 562   |
|                  | percentage = 0.3, $\kappa = 1$ | $0.96 \pm 0.19$ | 2.75              | 1226  |
|                  | percentage = 1.0, $\kappa = 1$ | $0.99 \pm 0.09$ | 3.11              | 1400  |
|                  | percentage = 1.0, $\kappa = 3$ | $1.0 \pm 0.0$   | 3.75              | 1854  |

### B.11.2 Investigation on automatic thinking assignment across different difficulty levels

The Figure 15 visualize how our method allocates varying amounts of inference iterations and time depending on task difficulty for Pixel Maze. It demonstrates that, similar to Sudoku, the model adaptively assigns greater computational effort to larger and more complex mazes, confirming the generality of adaptive inference-time allocation across domains.

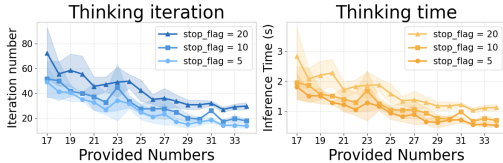


**Figure 14: Thinking iterations and inference time in Sudoku.** **Left:** Mean and standard deviation of iteration counts across varying numbers of provided digits. **Right:** Mean and standard deviation of per-instance inference time. The model adapts computation dynamically, allocating more iterations to harder puzzles with fewer initial clues.

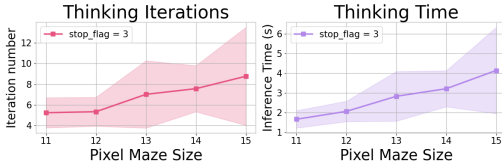


**Figure 15: Thinking iterations and inference time in Pixel Maze.** **Left:** Mean and standard deviation of iteration counts across different maze sizes. **Right:** Mean and standard deviation of per-sample inference time. Larger mazes require more search, and the model allocates compute accordingly, demonstrating instance-aware inference adaptation.

### B.12 Molecular 3D structure prediction task experiment detail

Experiments were conducted on 100 molecules randomly sampled from the QM9 test dataset. For all methods, we utilized the same checkpoint of diffusion model from the official EDM repository, where  $T = 1000$ . Following [11], we compared molecule stability (the proportion of generated molecules for which all atoms are stable). We also measured the average inference time required for a single sample.

To compare inference-time scaling strategies, each baseline was scaled along its primary computational axis while preserving its core algorithmic behavior. **Base Diffusion** employed a single particle ( $N = 1$ ). **BoN** was evaluated with using more  $N$  to increase inference cost. **BS** and **SoP** were implemented with  $M = 4$  and  $K = 10$ , and inference-time compute was scaled by increasing the branching and selection frequency. Specifically, for **BS**, we scale inference-time compute by adjusting the branching-and-selection frequency  $p$ . **SoP** additionally scaled computation by reducing the step sizes for back-and-forth moves  $\Delta f$  and  $\Delta b$ . **SMC** used  $N = 40$  particles and increased inference-time compute by adjusting the resampling frequency  $p$  over different steps. Following the FKD [24], we use POTENTIAL TYPE = "max" and  $\lambda = 100$  to make it as optimization. **ABCD (ours)** was configured with  $N = 10$ ,  $K = 10$ , and  $J = 5$ , corresponding to four non-zero go-back noise levels (50, 100, 200, 400) and a zero level. The adaptive terminal condition halted inference once a specified fraction of top- $N$  particles repeatedly originated from the zero noise level for  $\kappa$  consecutive steps. We scaled ABCD’s inference time by varying both  $\kappa \in \{1, 2\}$  and percentage thresholds  $\in \{0.4, 0.5\}$ . To ensure computational efficiency, ABCD employed 100 denoising steps, each executing a 10-step jump in the diffusion process.



### B.13 Molecular 3D structure prediction task experiment result

We provide detailed results corresponding to the main Figure 4(Right), with a breakdown of the scaling factors we used in Table 7.

**Table 7:** Comparison of various inference-time strategies across compute and performance in the QM9 setting.

| Inference Method | Add. Compute                     | Success rate | Clock Time (sec.) | NFE    |
|------------------|----------------------------------|--------------|-------------------|--------|
| Base Diffusion   | No add                           | 0.74         | 4.07              | 1001   |
| BoN              | N = 40                           | 0.86         | 17.33             | 40040  |
|                  | N = 80                           | 0.86         | 35.58             | 80080  |
|                  | N = 160                          | 0.89         | 70.28             | 160160 |
| SMC              | $p = 1$                          | 0.88         | 24.17             | 48040  |
|                  | $p = 2$                          | 0.85         | 35.18             | 60040  |
|                  | $p = 5$                          | 0.9          | 52.29             | 80010  |
| BS               | $p = 1$                          | 0.82         | 24.17             | 24010  |
|                  | $p = 2$                          | 0.83         | 37.95             | 45010  |
|                  | $p = 5$                          | 0.91         | 69.95             | 80010  |
| SoP              | $\Delta f = 50, \Delta b = 25$   | 0.9          | 32.21             | 73690  |
|                  | $\Delta f = 100, \Delta b = 50$  | 0.92         | 40.06             | 74410  |
|                  | $\Delta f = 200, \Delta b = 100$ | 94           | 49.84             | 75850  |
| ABCD             | percentage = 0.4, $\kappa = 1$   | 0.93         | 4.35              | 7482   |
|                  | percentage = 0.4, $\kappa = 2$   | 0.97         | 23.09             | 43009  |
|                  | percentage = 0.5, $\kappa = 2$   | 0.99         | 46.45             | 82010  |

### B.14 Text-to-image generation experiment detail

We adopt Stable Diffusion v1.5, a widely used text-to-image diffusion model, as our pre-trained model. we comprehensively assessed ABCD’s performance using three metrics: compressibility, measured as negative JPEG file size (in kilobytes) after compression following [2]; aesthetic evaluation, computed using LAION’s V2 Aesthetic Predictor [22], a linear MLP built upon CLIP embeddings, trained on over 400,000 human ratings; and human preference evaluation, based on the HPSv2 scorer [33], a CLIP model fine-tuned on 798,090 human-selected rankings across 433,760 image pairs. For compressibility and aesthetic evaluations, we used animal category prompts from [2] (e.g., Dog, Cat, Panda), whereas for human preference evaluation we used human instruction prompts from [33].

Each inference method is evaluated by generating 12 images. Inference time is calculated as the average duration to produce one image. To analyze inference-time scaling, each baseline method was scaled by adjusting its primary computational parameters without altering its fundamental algorithmic design. **Base Diffusion** utilized a single particle ( $N = 1$ ). **BoN** scaled inference by incrementing particle count from  $N = 2$  up to  $N = 12$ . **SoP** increased computational cost through smaller incremental steps during both forward and backward transitions, denoted by  $(\Delta f, \Delta b)$ . Our proposed **ABCD** method employed  $N = 4, K = 1$ , and  $J = 4$ , translating to three non-zero noise levels (1, 301, 621) for backward transitions and one zero-noise level. The adaptive stopping criterion halted inference when the top-K particles persistently emerged from the zero noise level for  $\kappa = 30$  consecutive steps. ABCD’s inference scaling was achieved by varying the number of `max_iter`. For fast denoising, ABCD employed 50 inference steps with each step covering a 20-step jump in the diffusion space. Detailed results are provided in the next section B.15.

### B.15 Text-to-image generation experiment result

We present detailed results related to Figure 7 along with a breakdown of the scaling factors listed in Table 8, Table 9 and Table 10. For each method, inference-time compute was scaled by adjusting its primary control axis while preserving its core algorithmic behavior.

**Table 8:** Comparison of various inference-time strategies across compute and image compressibility in the Text-to-image generation task.

| Inference Method | Add. Compute                     | Compressibility    | Clock Time (sec.) | NFEs  |
|------------------|----------------------------------|--------------------|-------------------|-------|
| Base Diffusion   | No add                           | $-100.07 \pm 2.88$ | 58.42             | 2000  |
| BoN              | N = 2                            | $-91.59 \pm 4.43$  | 109.25            | 4000  |
|                  | N = 3                            | $-83.70 \pm 7.60$  | 150.17            | 6000  |
|                  | N = 4                            | $-81.89 \pm 5.71$  | 200.00            | 8000  |
|                  | N = 5                            | $-81.89 \pm 5.71$  | 257.58            | 10000 |
|                  | N = 6                            | $-81.64 \pm 5.92$  | 292.75            | 12000 |
|                  | N = 7                            | $-78.21 \pm 8.68$  | 348.33            | 14000 |
|                  | N = 8                            | $-78.22 \pm 8.69$  | 403.00            | 16000 |
|                  | N = 9                            | $-78.00 \pm 8.40$  | 444.58            | 18000 |
|                  | N = 10                           | $-77.86 \pm 8.42$  | 494.33            | 20000 |
|                  | N = 11                           | $-77.53 \pm 8.77$  | 556.33            | 22000 |
|                  | N = 12                           | $-77.02 \pm 8.88$  | 583.25            | 24000 |
| SoP              | $\Delta f = 510, \Delta b = 255$ | $-88.36 \pm 4.88$  | 188.75            | 7548  |
|                  | $\Delta f = 410, \Delta b = 205$ | $-85.32 \pm 3.21$  | 215.50            | 8490  |
|                  | $\Delta f = 350, \Delta b = 175$ | $-80.82 \pm 4.14$  | 227.92            | 9192  |
|                  | $\Delta f = 280, \Delta b = 140$ | $-72.64 \pm 5.61$  | 257.67            | 10266 |
|                  | $\Delta f = 220, \Delta b = 110$ | $-67.79 \pm 4.65$  | 271.25            | 10710 |
|                  | $\Delta f = 180, \Delta b = 90$  | $-64.59 \pm 3.43$  | 280.25            | 10974 |
| ABCD             | max_iter = 10                    | $-74.91 \pm 5.58$  | 41.83             | 1380  |
|                  | max_iter = 20                    | $-67.19 \pm 5.84$  | 73.67             | 2360  |
|                  | max_iter = 30                    | $-62.33 \pm 4.33$  | 103.67            | 3340  |
|                  | max_iter = 40                    | $-59.01 \pm 4.34$  | 130.50            | 4320  |
|                  | max_iter = 50                    | $-56.08 \pm 4.02$  | 163.67            | 5300  |
|                  | max_iter = 80                    | $-51.49 \pm 4.34$  | 254.50            | 8240  |
|                  | max_iter = 100                   | $-49.17 \pm 4.29$  | 306.08            | 10176 |

**Table 9:** Comparison of various inference-time strategies across compute and aesthetic score in the Text-to-image generation task.

| Inference Method | Add. Compute                     | Image Aesthetic | Clock time (sec.) | NFEs  |
|------------------|----------------------------------|-----------------|-------------------|-------|
| Base Diffusion   | No add                           | $5.57 \pm 0.03$ | 58.83             | 2000  |
| BoN              | N = 2                            | $5.63 \pm 0.08$ | 109.75            | 4000  |
|                  | N = 3                            | $5.72 \pm 0.09$ | 150.92            | 6000  |
|                  | N = 4                            | $5.75 \pm 0.07$ | 200.58            | 8000  |
|                  | N = 5                            | $5.79 \pm 0.05$ | 258.33            | 10000 |
|                  | N = 6                            | $5.81 \pm 0.02$ | 293.42            | 12000 |
|                  | N = 7                            | $5.81 \pm 0.02$ | 349.00            | 14000 |
|                  | N = 8                            | $5.82 \pm 0.03$ | 403.50            | 16000 |
|                  | N = 9                            | $5.86 \pm 0.05$ | 445.25            | 18000 |
|                  | N = 10                           | $5.86 \pm 0.05$ | 494.25            | 20000 |
|                  | N = 11                           | $5.87 \pm 0.04$ | 556.75            | 22000 |
|                  | N = 12                           | $5.90 \pm 0.05$ | 583.17            | 24000 |
| SoP              | $\Delta f = 510, \Delta b = 255$ | $5.68 \pm 0.03$ | 189.42            | 7548  |
|                  | $\Delta f = 400, \Delta b = 200$ | $5.78 \pm 0.03$ | 206.83            | 9636  |
|                  | $\Delta f = 280, \Delta b = 140$ | $5.84 \pm 0.08$ | 258.67            | 10266 |
|                  | $\Delta f = 170, \Delta b = 85$  | $5.87 \pm 0.04$ | 285.08            | 10704 |
|                  | $\Delta f = 130, \Delta b = 65$  | $5.93 \pm 0.08$ | 301.42            | 11232 |
|                  | $\Delta f = 110, \Delta b = 55$  | $5.98 \pm 0.02$ | 313.67            | 11478 |
| ABCD             | max_iter = 10                    | $5.95 \pm 0.06$ | 40.00             | 1380  |
|                  | max_iter = 20                    | $6.08 \pm 0.06$ | 72.17             | 2360  |
|                  | max_iter = 30                    | $6.13 \pm 0.09$ | 105.42            | 3340  |
|                  | max_iter = 40                    | $6.15 \pm 0.08$ | 132.00            | 4254  |
|                  | max_iter = 60                    | $6.18 \pm 0.05$ | 178.75            | 6043  |
|                  | max_iter = 80                    | $6.23 \pm 0.07$ | 233.83            | 7677  |
|                  | max_iter = 100                   | $6.25 \pm 0.09$ | 288.42            | 9147  |

**Table 10:** Comparison of various inference-time strategies across compute and human preference score in the Text-to-image generation task.

| Inference Method | Add. Compute                     | Human Preference    | Clock time (sec.) | NFEs  |
|------------------|----------------------------------|---------------------|-------------------|-------|
| Base Diffusion   | No add                           | $0.2710 \pm 0.0028$ | 61.00             | 2000  |
| BoN              | N = 2                            | $0.2749 \pm 0.0013$ | 112.25            | 4000  |
|                  | N = 3                            | $0.2752 \pm 0.0017$ | 153.00            | 6000  |
|                  | N = 4                            | $0.2752 \pm 0.0018$ | 203.08            | 8000  |
|                  | N = 5                            | $0.2753 \pm 0.0017$ | 260.92            | 10000 |
| SoP              | $\Delta f = 510, \Delta b = 255$ | $0.2725 \pm 0.0031$ | 192.83            | 7548  |
|                  | $\Delta f = 410, \Delta b = 205$ | $0.2728 \pm 0.0030$ | 221.00            | 8490  |
|                  | $\Delta f = 350, \Delta b = 175$ | $0.2739 \pm 0.0044$ | 233.00            | 9192  |
|                  | $\Delta f = 230, \Delta b = 115$ | $0.2751 \pm 0.0029$ | 272.25            | 10218 |
|                  | $\Delta f = 130, \Delta b = 65$  | $0.2765 \pm 0.0046$ | 811.25            | 11232 |
|                  | $\Delta f = 70, \Delta b = 35$   | $0.2777 \pm 0.0039$ | 335.42            | 11778 |
|                  | $\Delta f = 20, \Delta b = 10$   | $0.2787 \pm 0.0027$ | 431.42            | 13056 |
| ABCD             | max_iter = 10                    | $0.2776 \pm 0.0027$ | 46.83             | 1380  |
|                  | max_iter = 20                    | $0.2791 \pm 0.0021$ | 82.83             | 2360  |
|                  | max_iter = 30                    | $0.2797 \pm 0.0023$ | 115.92            | 3340  |
|                  | max_iter = 40                    | $0.2804 \pm 0.0027$ | 142.17            | 4320  |
|                  | max_iter = 50                    | $0.2808 \pm 0.0028$ | 183.42            | 5300  |
|                  | max_iter = 80                    | $0.2815 \pm 0.0030$ | 272.08            | 8060  |
|                  | max_iter = 100                   | $0.2819 \pm 0.0032$ | 322.08            | 9718  |
|                  | max_iter = 200                   | $0.2823 \pm 0.0033$ | 432.92            | 12716 |

### B.15.1 Visualization of generated images

In this section, we show more generated samples. Figures 16, 17, and 18 compare outputs from baseline approaches and ABCD with respect to compressibility, aesthetic score, and human preference score, respectively.

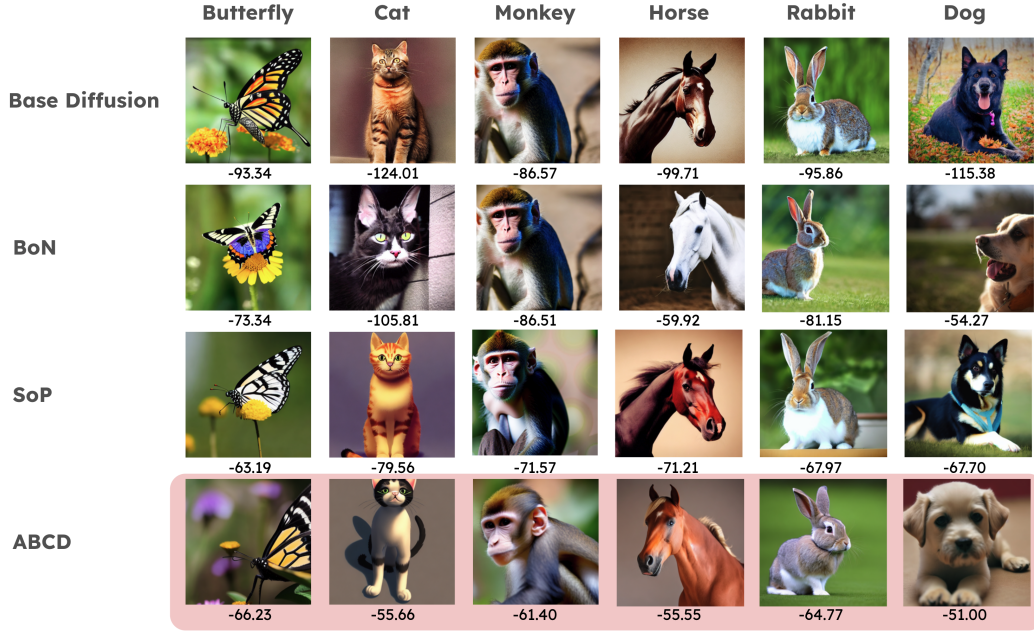


**Figure 16: Visual comparison of images produced by different inference-time strategies optimizing compressibility reward.** Numbers at the bottom of each image show the corresponding compressibility scores. **Base Diffusion** produces photorealistic textures and complex backgrounds, but at the cost of very large file sizes. **BoN** occasionally yields simpler backgrounds but still leaves a lot of high-frequency detail. **SoP** further flatten color gradients, shaving further off file size. Under **ABCD**, each image sports a clean, uncluttered background and smoother regions—e.g., the Cat is rendered with minimal fur grain, the Horse with a crisp silhouette against a solid tone.

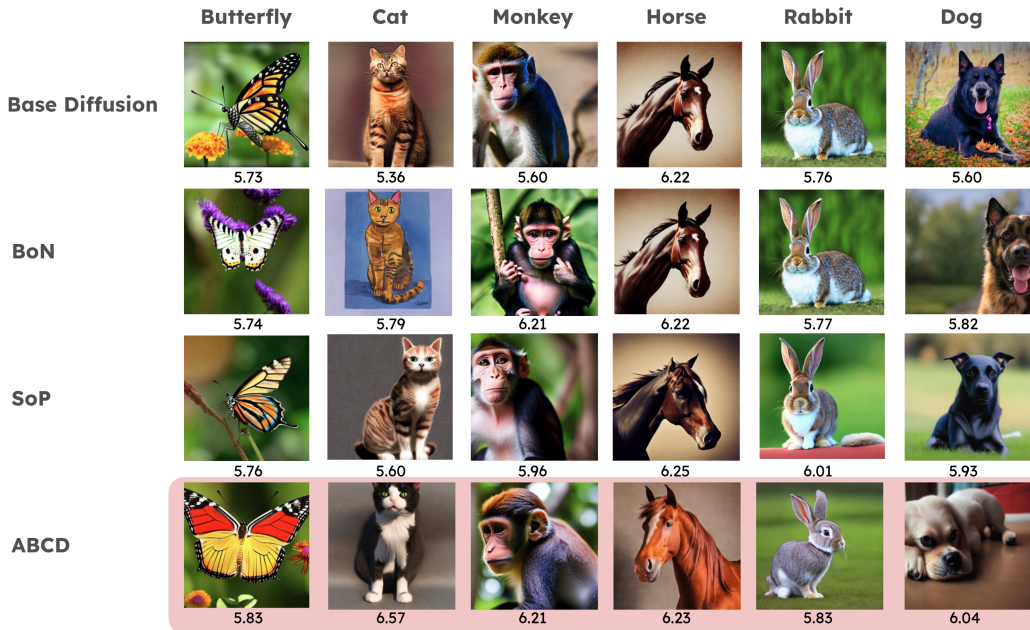


**Figure 17: Visual comparison of images produced by different inference-time strategies optimizing aesthetic score reward.** Numbers at the bottom of each image show the corresponding aesthetic scores.



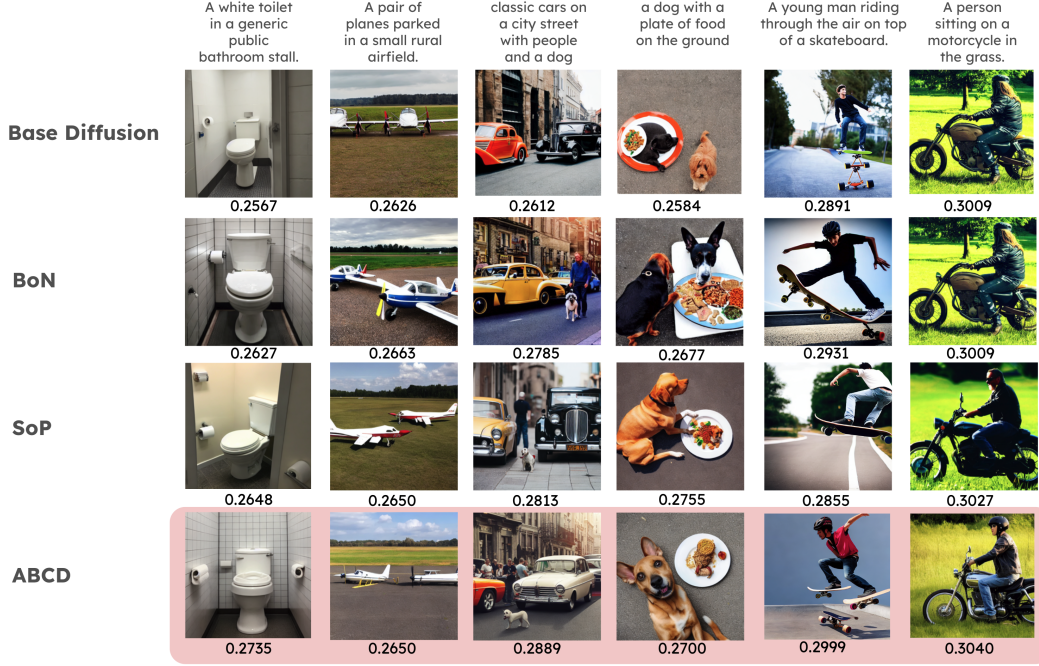


**Figure 18: Visual comparison of images produced by different inference-time strategies optimizing human preference score reward.** Numbers at the bottom of each image show the corresponding human preference scores.

#### B.16 Comparison with respect to number of function evaluations of the diffusion model

In this section, we present a more detailed and fair comparison with baselines by evaluating not only the wall-clock time but also the Number of Function Evaluations (NFEs) during inference across tasks. The NFE measures how many times the pretrained diffusion function is called, and to isolate pure computational cost from parallelization effects, we count one function evaluation per particle per step. As shown in Figure 19, ABCD demonstrates superior inference-time scaling compared to other baselines, consistent with wall-clock time results.

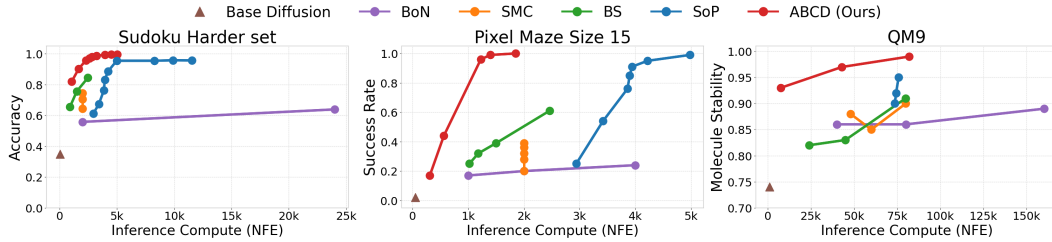


**Figure 19: Comparison w.r.t NFEs. Left:** Mean accuracy on Sudoku Harder dataset (17-28 entities provided). **Middle:** Pixel maze path finding result. (Size 15). Success rate on the OOD size-15 pixel maze test set. **Right:** Molecular 3D structure prediction task result. Molecular Stability rate on the QM9 dataset.

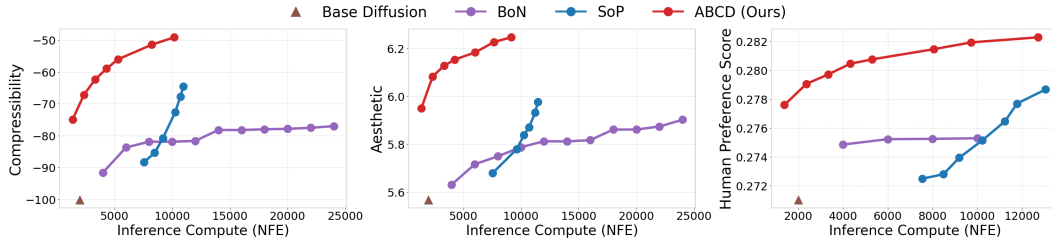


**Figure 20: Comparison w.r.t NFEs on Text-to-Image generation task.** Text-to-image generation result. Average reward with respect to compressibility, aesthetic score and human preference score.

## C Ablation studies

### C.1 Investigate on existence of inference time scalable *go-back* noise level per task

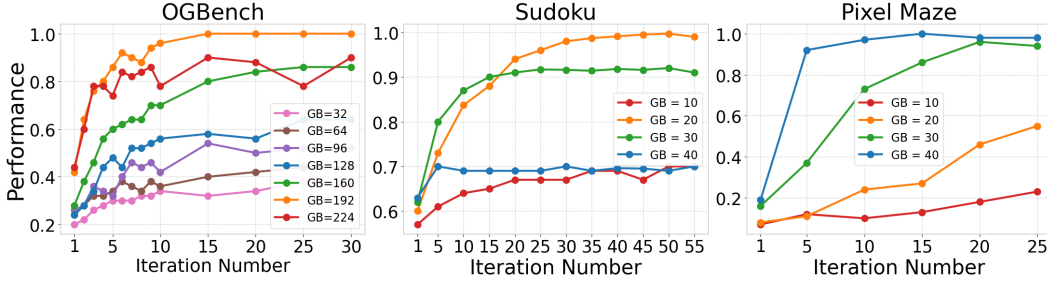


**Figure 21: Existence of Inference-Time Scalable *go-back* Noise Level per Task.** Left: OGBench Point Maze Giant. Middle: Sudoku harder dataset (17 to 34 provided). Right: Pixel Maze (Size 15). Performance across iterations for different *go-back* noise levels. Each task exhibits a distinct optimal *go-back* level, demonstrating the necessity of task-specific noise-level selection for effective inference-time scaling.

**Existence of inference time scalable *go-back* noise level per tasks.** To investigate the impact of the *go-back* noise level on inference-time scaling, we conducted an additional study across OGBench Point Maze, Sudoku, and Pixel Maze. As shown in Figure 21, the optimal *go-back* noise level—expressed as a fraction of the total denoising steps—varies significantly across tasks: approximately 3/4 for OGBench, 2/5 for Sudoku, and 4/5 for Pixel Maze. These results highlight that selecting an appropriate *go-back* step size is critical for effective iterative refinement during inference time.

### C.2 Investigate on different configuration of Adaptive Thinking Time

**As the terminal condition becomes more stringent, both performance and inference cost increase.** To better understand how different computational budgets affect final performance, we added ablation study analyzing the core components of ABCD—Adaptive Thinking Time and Automatic Exploration-Exploitation Balancing—under varying configurations. Specifically, we conducted experiments that vary the level of computation allocated to each mechanism to examine how efficiency and accuracy are impacted in both the Sudoku and text-to-image generation domains.

In the Sudoku task, We focused on the Adaptive Thinking Time mechanism by varying the termination percentage and the value of  $\kappa$ , two key hyperparameters that define ABCD’s adaptive terminal condition. As shown in the two tables 11, 12, increasing  $\kappa$  generally improves accuracy but also leads to longer inference time, and similarly, raising the termination percentage improves performance at the cost of additional computation. These results show that by adjusting the strictness of the termination criterion, we can effectively control the trade-off between accuracy and efficiency.

**Table 11: ABCD – Sudoku (Changing  $\kappa$ ).** We report accuracy, wall-clock time, and NFEs under different  $\kappa$  values.

| Metric   | $\kappa = 1$ | $\kappa = 5$ | $\kappa = 10$ |
|----------|--------------|--------------|---------------|
| Accuracy | 0.958        | 0.986        | 0.994         |
| Time (s) | 0.443        | 0.608        | 0.754         |
| NFEs     | 2296         | 3205         | 3942          |

**Table 12: ABCD – Sudoku (Changing percentage).** We report accuracy, wall-clock time, and NFEs under different percentage values.

| Metric   | perc=0.4 | perc=0.6 | perc=0.8 |
|----------|----------|----------|----------|
| Accuracy | 0.698    | 0.821    | 0.903    |
| Time (s) | 0.112    | 0.210    | 0.329    |
| NFEs     | 520      | 1059     | 1667     |

In the text-to-image generation task, we analyzed the Automatic Exploration-Exploitation Balancing mechanism by varying the granularity of the temperature pool—specifically, the number of *go-back* temperatures included in the pool. We fixed the number of particles and terminal conditions ( $\text{max\_iter}=50$ ,  $\kappa = 30$ ) and varied the temperature pool size. As shown in the two tables 13, 14, using a finer pool (i.e., more diverse temperature values) improves the final compressibility and aesthetic score but also increases both inference time and NFE. This experiment highlights the impact of temperature diversity on controllability and performance.

**Table 13: More diverse temperature values on Compressibility score.** We report Compressibility score, wall-clock time, and NFEs under different temperature pool size.

| $\mathcal{T}$ size | Comp            | Time (s) | NFEs  |
|--------------------|-----------------|----------|-------|
| 2                  | -55.1 $\pm$ 4.9 | 233.3    | 8188  |
| 3                  | -48.8 $\pm$ 2.1 | 285.8    | 10500 |
| 4                  | -46.1 $\pm$ 2.1 | 356.5    | 12800 |

**Table 14: More diverse temperature values on Aesthetic score.** We report Aesthetic score, wall-clock time, and NFEs under different temperature pool size.

| $\mathcal{T}$ size | Aesth           | Time (s) | NFEs  |
|--------------------|-----------------|----------|-------|
| 2                  | 6.23 $\pm$ 0.05 | 237.9    | 8200  |
| 3                  | 6.31 $\pm$ 0.04 | 286.5    | 10369 |
| 4                  | 6.36 $\pm$ 0.14 | 354.6    | 12578 |

### C.3 Comparison with more intelligent *go-back* strategy

Since some amount of unnecessary compute is being performed by distributing each sample uniformly along the noise levels, we explored a more intelligent go-back strategy—Adaptive ABCD—but found it doesn’t show meaningful improvement. Specifically, we tested strategy where particles were redistributed to different noise levels in proportion to the average reward observed at those levels across the population. However, as shown in the table [15](#) despite its intuitive appeal, the performance improvement was marginal compared to the added complexity. Therefore, we ultimately chose a simpler and more efficient formulation for the current version of ABCD. Nevertheless, we believe that incorporating smarter strategies—such as applying ideas from SMC to the temperature pool—could be a promising direction.

**Table 15:** Comparison between Adaptive ABCD and ABCD. We report accuracy and wall-clock time under different compute configurations.

| Method               | Add. Compute          | Accuracy | Wall Clock Time (s) |
|----------------------|-----------------------|----------|---------------------|
| <b>Adaptive ABCD</b> | perc=0.6, $\kappa$ =1 | 0.810    | 0.220               |
|                      | perc=0.8, $\kappa$ =1 | 0.895    | 0.395               |
|                      | perc=1.0, $\kappa$ =1 | 0.951    | 0.489               |
|                      | perc=1.0, $\kappa$ =3 | 0.979    | 0.549               |
| <b>ABCD</b>          | perc=0.6, $\kappa$ =1 | 0.821    | 0.240               |
|                      | perc=0.8, $\kappa$ =1 | 0.903    | 0.350               |
|                      | perc=1.0, $\kappa$ =1 | 0.958    | 0.450               |
|                      | perc=1.0, $\kappa$ =3 | 0.979    | 0.557               |

#### C.4 Investigate on the diversity preservation of ABCD

We measured diversity using the average pairwise cosine similarity of CLIP embeddings, where a lower score reflects greater variability in outputs and broader exploration of the data space. While optimization naturally reduces some diversity, our method successfully preserves the underlying multi-modality of the pretrained model while steering toward high-reward regions.

**Table 16: Comparison of diversity scores across Compressibility, Aesthetic, and HPS tasks.** We report the diversity mean  $\pm$  std under different compute configurations.

| Method         | Add compute                  | Compressibility                     | Aesthetic                           | HPS                                 |
|----------------|------------------------------|-------------------------------------|-------------------------------------|-------------------------------------|
| Base Diffusion | -                            | 0.2957 $\pm$ 0.0481                 | 0.2957 $\pm$ 0.0481                 | 0.4559 $\pm$ 0.0215                 |
| BoN            | N=5                          | 0.2859 $\pm$ 0.0190                 | 0.2870 $\pm$ 0.0102                 | 0.4424 $\pm$ 0.0095                 |
|                | N=10                         | 0.2781 $\pm$ 0.0184                 | 0.2919 $\pm$ 0.0285                 | -                                   |
| SoP            | $\Delta f=510, \Delta b=255$ | 0.2795 $\pm$ 0.0375                 | 0.2912 $\pm$ 0.0308                 | 0.4677 $\pm$ 0.0227                 |
|                | $\Delta f=280, \Delta b=140$ | 0.2975 $\pm$ 0.0512                 | 0.3005 $\pm$ 0.0199                 | -                                   |
|                | $\Delta f=230, \Delta b=115$ | -                                   | -                                   | 0.4508 $\pm$ 0.0152                 |
|                | $\Delta f=180, \Delta b=90$  | 0.2798 $\pm$ 0.0154                 | -                                   | -                                   |
|                | $\Delta f=170, \Delta b=85$  | -                                   | 0.2672 $\pm$ 0.0323                 | -                                   |
|                | $\Delta f=130, \Delta b=65$  | -                                   | -                                   | 0.4417 $\pm$ 0.0054                 |
| ABCD           | max_iter=30                  | 0.3128 $\pm$ 0.0084                 | 0.2848 $\pm$ 0.0221                 | <b>0.4672<math>\pm</math>0.0160</b> |
|                | max_iter=80                  | <b>0.3162<math>\pm</math>0.0028</b> | <b>0.2888<math>\pm</math>0.0222</b> | 0.4543 $\pm$ 0.0143                 |
|                | max_iter=100                 | 0.3037 $\pm$ 0.0171                 | 0.2880 $\pm$ 0.0242                 | 0.4555 $\pm$ 0.0167                 |

## D Prediction visualization

In this section, we provide illustrative visualizations of instance-level predictions generated by our model to facilitate intuitive understanding. Figure 22 displays representative outputs from both the Pixel Maze and Sudoku tasks.

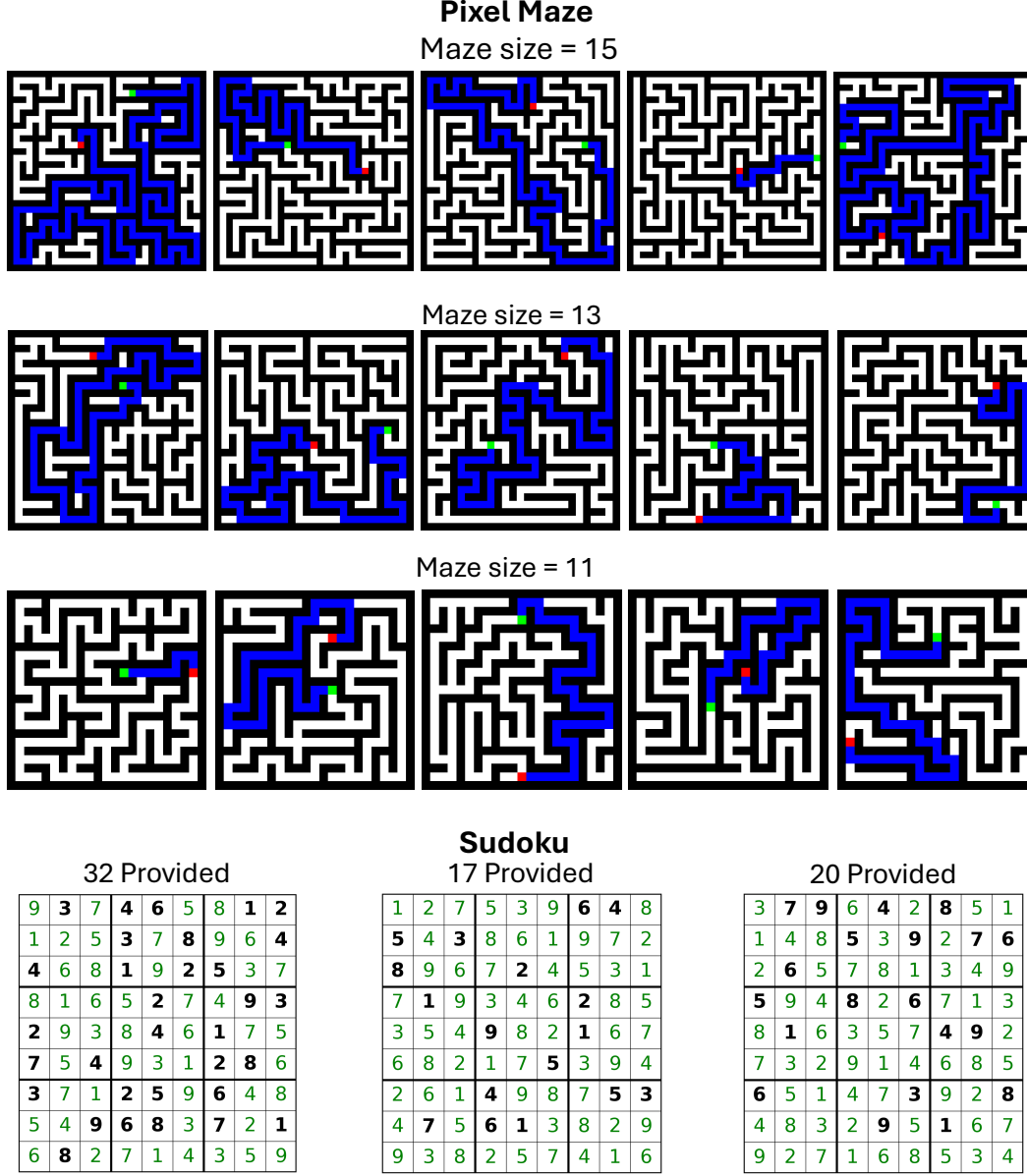


**Figure 22:** This figure presents the final outputs obtained by our ABCD method on both the Pixel Maze and Sudoku tasks. The visualizations demonstrate that, across a range of maze sizes and Sudoku difficulty levels, ABCD produces accurate predictions, particularly in instances that demand greater computational effort.



## E Termination guarantee of the Adaptive Thinking Time

In this section, we present a detailed proof establishing the termination guarantee of the Adaptive Thinking Time algorithm introduced in Section [3.3](#).

### E.1 Formal statement

Let

$$T = \{t_1, \dots, t_m\}$$

be the “temperature pool” with lowest temperature  $t_1 = 0$ . At cycle  $c$ , let  $D_k(c)$  be the multiset of origin-temperatures of the top- $k$  particles after denoising. Define the stopping rule: terminate at the first cycle  $N$  such that

$$\forall i \in \{N - \kappa + 1, \dots, N - 1, N\}, \quad D_k(i) = \{0, 0, \dots, 0\},$$

i.e. all top- $k$  particles originate from  $t_1 = 0$  for  $\kappa$  consecutive cycles.

#### Assumptions

1. **Bounded reward.** There is a reward function  $r : \mathbb{R}^d \rightarrow \mathbb{R}$  with finite supremum  $r^* < \infty$ .
2. **Monotonic selection.** Let

$$r_k(c) = \min\{\text{rewards of top-}k \text{ at cycle } c\}.$$

Then  $r_k(c)$  is non-decreasing in  $c$ .

3. **Attainment.** There exists at least one state  $x^*$  such that  $r(x^*) = r^*$ .

**Theorem 1.** *Under these assumptions, ABCD’s Adaptive Thinking Time criterion triggers termination in finite time.*

The proof of this theorem is built upon several key lemmas, which we will now introduce and prove.

### E.2 Uniform Hit-Chance

**Lemma E.1.** *Let  $x^*$  be any maximizer of the reward,  $r(x^*) = r^*$ . Under the ABCD dynamics (Algorithm [1](#)), there is a constant  $p > 0$  such that for each cycle  $c$ ,*

$$\Pr(E_c \mid \mathcal{F}_{c-1}) \geq p,$$

where  $E_c = “x^* \text{ appears among the selected top-}K \text{ at cycle } c”$  and  $\mathcal{F}_{c-1}$  is the  $\sigma$ -algebra of all randomness up to (but not including) cycle  $c$ .

*Proof.* 1. At the start of cycle  $c$  we have  $K$  anchor particles at  $t = 0$ . We replicate each  $J$  times and send each of those  $KJ$  copies through the forward noising process  $q(x_{t'} \mid x_0)$  at every  $t' \in T$ . Exactly  $K$  of those replicas go to the highest temperature  $t_m$ .

2. Conditioned on  $\mathcal{F}_{c-1}$ , the noising and denoising of these  $KJ$  particles is independent of the past and identically distributed across cycles. In particular, the  $K$  samples at  $t_m$  are fresh each time. Let

$$q = \Pr[(\text{noising at } t_m) \text{ then (denoise) yields } x^*].$$

By full support of the forward kernel and nonzero recovery probability of the denoiser,  $q > 0$ .

3. Those  $K$  draws at  $t_m$  are independent, so the chance none equals  $x^*$  is  $(1 - q)^K$ . Hence

$$p = 1 - (1 - q)^K > 0.$$

4. If any replicate equals  $x^*$ , its reward is  $r^*$ , guaranteeing  $x^*$  is in the top- $K$ . Thus for every history,

$$\Pr(E_c \mid \mathcal{F}_{c-1}) = \Pr(\text{some } t_m\text{-replicate} = x^* \mid \mathcal{F}_{c-1}) \geq p.$$

This completes the proof of the uniform hit-chance lemma.  $\square$

### E.3 Optimality

**Lemma E.2.** *Under the assumptions*

1. Monotonicity and Boundedness:  $r_k(c)$  is non-decreasing and  $r_k(c) \leq r^* < \infty$ , so  $r_k(c) \rightarrow r_\infty \leq r^*$ .
2. Supremum Attained:  $\exists x^*$  with  $r(x^*) = r^*$ .
3. Uniform Hit-Chance: at each cycle  $c$ ,  $\Pr(E_c \mid \text{past}) \geq p > 0$ .

Then

$$\Pr[r_\infty = r^*] = 1.$$

- Proof.* 1. Define the “hit” event  $E_c$  as above. By assumption 3,  $\sum_{c=1}^{\infty} \Pr(E_c \mid \text{past}) \geq \sum_c p = \infty$ .
2. By the conditional Borel–Cantelli lemma [23],  $\Pr(E_c \text{ i.o.}) = 1$ , so infinitely many hits occur almost surely.
3. Let  $C$  be the first cycle where  $E_C$  occurs. Then

$$r_k(C) \geq r(x^*) = r^*, \quad r_k(C) \leq r^*, \quad \implies \quad r_k(C) = r^*.$$

4. Monotonicity then implies  $r_k(c) = r^*$  for all  $c \geq C$ , so  $r_\infty = r^*$ .

Hence  $\Pr[r_\infty = r^*] = 1$ . □

### E.4 Finite-Time Hitting

**Lemma E.3.** *Under the Uniform Hit-Chance lemma, define*

$$T = \inf\{c \geq 1 \mid x^* \text{ appears among the top-}K \text{ at cycle } c\}.$$

Then

$$\Pr(T < \infty) = 1, \quad \Pr(T > n) \leq (1 - p)^n \quad \forall n \in \mathbb{N},$$

where  $p > 0$  is the per-cycle success lower bound.

*Proof.* 1. **Failure-to-hit bound.**

Let

$$F_n = \bigcap_{c=1}^n E_c^c, \quad E_c = \{\text{cycle } c \text{ hits } x^*\}.$$

By the Uniform Hit-Chance lemma,

$$\Pr(E_c \mid \mathcal{F}_{c-1}) \geq p \implies \Pr(E_c^c \mid \mathcal{F}_{c-1}) \leq 1 - p.$$

Hence, by the tower property,

$$\Pr(F_n) = \Pr(E_1^c \cap \dots \cap E_n^c) = \mathbb{E}[\Pr(E_n^c \mid \mathcal{F}_{n-1}) \mathbf{1}_{F_{n-1}}] \leq (1 - p) \Pr(F_{n-1}),$$

and by induction

$$\Pr(F_n) \leq (1 - p)^n.$$

2. **Hitting in finite time w.p.1.**

Since  $\{T > n\} = F_n$ , we get

$$\Pr(T > n) \leq (1 - p)^n \xrightarrow{n \rightarrow \infty} 0,$$

so  $\Pr(T = \infty) = 0$  and hence  $\Pr(T < \infty) = 1$ . □

## E.5 Proof of Main Theorem

We now assemble the results from the lemmas to prove Theorem [I](#).

1. **Monotone convergence of  $r_k(c)$ .** The sequence  $r_k(0), r_k(1), r_k(2), \dots$  is non-decreasing and bounded above by  $r^*$ , hence it converges to some limit  $r_\infty \leq r^*$ .
2. **Limit must equal  $r^*$ .** According to Lemma [E.2](#)  $r_\infty = r^*$ .
3. **Optimal is reached in finite time.** By Lemma [E.3](#)  $r_k(c)$  hits  $r^*$  at some finite cycle  $C$ .
4. **Once optimal is reached, only  $t_1$ -origins survive.** At cycle  $C$  where  $r_k(C) = r^*$ , any particle noised at temperatures  $t > 0$  and then denoised back cannot exceed  $r^*$ . Thus the only way to preserve the top- $k$  set of reward- $r^*$  particles is via replicas from  $t_1 = 0$ , which leave them unchanged. Consequently, for all  $c \geq C$ ,  $D_k(c) = \{0, 0, \dots, 0\}$ .
5.  **$\kappa$ -persistence triggers termination.** Therefore, once cycle  $C$  is reached, the condition “all top- $k$  from temperature 0 for  $\kappa$  consecutive cycles” is satisfied by cycle  $C + \kappa - 1$ , and ABCD terminates.